Direct evidence of heterogeneous mechanical relaxation in supercooled liquids

Akira Furukawa[*] and Hajime Tanaka

Institute of Industrial Science, University of Tokyo, Meguro-ku, Tokyo 153-8505, Japan
(Received 21 January 2011; revised manuscript received 19 September 2011; published 14 December 2011)

Dynamic heterogeneity is now considered to be an intrinsic kinetic feature of a supercooled liquid. Here, we access the nonlocal complex modulus of a glass-forming liquid using molecular dynamics simulations. We find that the shear-stress relaxation exhibits a marked wave number dependence in a supercooled state. This dependence provides direct evidence that slow mechanical relaxation takes place heterogeneously in space. Its characteristic length ξ increases with decreasing temperature and becomes mesoscopic. The response involves particle rearrangements over ξ and takes a time comparable to the structural relaxation time τ_α. Our finding suggests that the heterogeneous structural relaxation is of fundamental importance in anomalous viscous transport and viscoelasticity in supercooled liquids.

I. INTRODUCTION

The viscosity η of a liquid increases steeply as it approaches the glass-transition temperature T_g. The origin of this viscous slowing down is the central issue of the physics of the glass transition [1–3]. Similarly, the α-relaxation time τ_α (the longest structural relaxation time) also increases. This τ_α can be accessed not only by macroscopic measurements such as mechanical and dielectric relaxation measurements, but also by microscopic measurements, such as neutron scattering measurements, and numerical simulations, which probe the decay of the density correlation function at the peak wave number k_p of the structure factor $S(k)$. Intriguingly, τ_α obtained by microscopic measurements ($k = k_p$) coincide with that obtained by macroscopic measurements ($k = 0$). Furthermore, τ_α is proportional to η. This proportionality is considered to be a consequence of the Maxwell relation $\eta = G_0 \tau_\alpha$, where G_0 is the plateau shear modulus. This link between the macroscopic η and τ_α at $k = 0$ and microscopic τ_α at k_p apparently suggests that the slow dynamics occur even at the microscopic scale, and thus have a microscopic origin. Mode coupling theory (MCT) provides a scenario that directly bridges the macroscopic and microscopic structural relaxations [4]. Within the framework of MCT, jamming of density fluctuations, whose characteristic length scale is the cage size ($\sim$ particle size d), is the essential origin of the excessive slowing down that identifies macroscopic structural relaxation. Because of this feature, MCT has been considered to be a microscopic (or first-principles) theory that can explain various key aspects of the glass transition.

In the last decade, however, this slow structural relaxation has been revealed to accompany dynamic heterogeneity (DH), and its characteristic length ξ grows as the system approaches T_g [5–15]. This property is now considered to be an intrinsic and universal kinetic feature of the glassy dynamics of a supercooled liquid. It is agreed by consensus that DH is responsible for many anomalous phenomena that are absent in a normal liquid but characteristic of a supercooled liquid. These phenomena include the nonexponential nature of the structural relaxation and the violation of the Stokes-Einstein

relation (translational-rotational decoupling) [16–18]. DH cannot be explained by the original MCT, in which the only relevant length scale is the microscopic cage size ($\sim d$), although there have been some efforts to incorporate spatially inhomogeneous dynamics by extending the original MCT (e.g., including higher order correlations [19] or hopping [20]). DH suggests the significance of dynamical correlation over a mesoscopic length scale ξ; therefore, the microscopic and mesoscopic length scales, d and ξ, are required to characterize the slow glassy dynamics of a supercooled liquid. This requirement raises the fundamental question of whether the spatial heterogeneity of structural relaxation is critical to viscous transport and slow glassy dynamics or merely a subsidiary phenomenon. This problem of the relevant length scale(s) of slow dynamics is crucial for the basic understanding of the origin of slow structural relaxation.

Recently, we studied the spatially nonlocal nature of viscous transport in a supercooled liquid [21]. We showed that a distinct crossover from the microscopic to macroscopic viscosity occurs at the dynamic correlation length ξ, which is comparable to the characteristic size of DH. It was also found that if the relaxation time of the longitudinal modes (e.g., density fluctuations) was substituted for that of the transverse shear stress, the Maxwell relation $\eta \cong G_0 \tau$ did not hold. In this paper, we investigate nonlocality in time and its link to spatial nonlocality to elucidate the physical origin behind these phenomena by accessing the viscoelastic shear response at a finite wave number k. We will demonstrate that, for $k\xi \gtrsim 1$, the structural relaxation linked to longitudinal modes is strongly decoupled from the shear mechanical relaxation, which involves only transverse modes. The fact that τ in the Maxwell relation $\eta = G_0 \tau$ should refer to the "transverse" shear relaxation time in principle and is much smaller than the macroscopic structural relaxation time, τ_α for $k\xi \gtrsim 1$, has been overlooked.

II. SIMULATION METHOD

In this paper, we performed molecular dynamics (MD) simulations of a three-dimensional (3D) glass-forming model liquid, focusing on its nonlocal viscoelastic response. The system used is a mixture of two types of particles, 1 and 2, with $N_1 = N_2 = 20\,000$. The particles interact by means of the

—————
[*]furu@iis.u-tokyo.ac.jp

soft-core potentials $U_{ab}(r) = \epsilon(d_{ab}/r)^{12}$ with $d_{ab} = (d_a + d_b)/2$, where r is the distance between two particles, d_a is the particle size, and $a,b = 1,2$. The mass and size ratios are $m_2/m_1 = 2$ and $d_2/d_1 = 1.2$, respectively. We fixed the particle number density at a value of $N/V = 0.8/d_1^3$, where $N = N_1 + N_2$, and V is the system volume. Space and time were measured in units of d_1 and $\tau_0 = (m_1 d_1^2/\epsilon)^{1/2}$, respectively. The linear dimension of the system was $L = 36.84$. The temperature T and viscosity η were measured in units of ϵ/k_B, where k_B is the Boltzmann constant, and $\epsilon\tau_0/d_1^3$, respectively. The simulations were carried out using velocity Verlet algorithms in the *NVE* ensemble [22].

III. MICRO- AND MACROSCOPIC α-RELAXATION TIMES IN A GLASS-FORMING LIQUID

In Fig. 1(a), we display the incoherent intermediate scattering function for species 1,

$$F_s^{(1)}(\boldsymbol{k}_0,t) = \frac{1}{N_1} \sum_{i=1}^{N_1} \langle e^{-i\boldsymbol{k}_0 \cdot \Delta \boldsymbol{r}_i^{(1)}(t)} \rangle, \qquad (1)$$

where $\Delta \boldsymbol{r}_i^{(1)}(t) = \boldsymbol{r}_i^{(1)}(t) - \boldsymbol{r}_i^{(1)}(0)$ and $|\boldsymbol{k}_0| = 2\pi$, which is nearly equal to k_p. Here, we define τ_α^s as $F_s^{(1)}(\boldsymbol{k}_0,\tau_\alpha) = e^{-1}$.

We also quantify DH and the associated correlated dynamics, following the method proposed in Ref. [13]: The mobility can be characterized by the time-dependent field variable

$$\hat{Q}(\boldsymbol{r},t) = \sum_{i=0}^{N} w_i(t)\delta(\boldsymbol{r} - \boldsymbol{r}_i(0)). \qquad (2)$$

Here, $w_i = w(|\boldsymbol{r}_i(t) - \boldsymbol{r}_i(0)|)$, where $w(|\boldsymbol{r}|) = 1$ for $|\boldsymbol{r}| \leqslant 0.3$ and $w(|\boldsymbol{r}|) = 0$ otherwise. The spatial integral $Q(t) = \int d\boldsymbol{r}\, \hat{Q}(\boldsymbol{r},t)$ counts the number of self-overlapping particles in two configurations separated by a time interval t. In Fig. 1(b), $\langle Q(t)/N \rangle$ is plotted for several temperatures, and its time evolution is found to be similar to that of $F_s^{(1)}(\boldsymbol{k}_0,t)$. We now define the relaxation time of the particle configuration, τ_α^Q, to be the time at which $\langle Q(t)/N \rangle$ is equal to e^{-1}. The mean square variance of $Q(t)$ measures the degree of cooperativity of the particle rearrangement dynamics:

$$\chi_4(t) = \frac{V}{TN^2}[\langle Q^2(t) \rangle - \langle Q(t) \rangle^2]. \qquad (3)$$

Figure 1(c) shows $\chi_4(t)$ for several temperatures. We estimate τ_χ to be the time at which $\chi_4(t)$ reaches its peak and thus the dynamic correlation becomes maximum.

First, we investigate the macroscopic ($k = 0$) viscoelastic relaxation and its relationship to other time scales characterizing the structural relaxation. The macroscopic shear viscosity can be obtained by the Green-Kubo formula:

$$\eta(k = 0) = \frac{1}{TV} \int_0^\infty dt \langle \hat{\sigma}_{xy}(t)\hat{\sigma}_{xy}(0) \rangle, \qquad (4)$$

where $\hat{\sigma}_{xy}(t)$ is the xy component of $\hat{\sigma}_{\boldsymbol{k}}(t)$ at $k = 0$. Here, $\hat{\sigma}_{\boldsymbol{k}}(t)$ is the Fourier component of the microscopic stress tensor, defined as follows [23,24]:

$$\hat{\sigma}_{\boldsymbol{k}}(t) = \sum_i \left[m_i \boldsymbol{v}_i \boldsymbol{v}_i + \sum_{j \neq i} \frac{\boldsymbol{r}_{ij}\boldsymbol{r}_{ij}}{r_{ij}^2} \Phi(\boldsymbol{r}_{ij}) \right] e^{-i\boldsymbol{k}\cdot\boldsymbol{r}_i(t)}, \qquad (5)$$
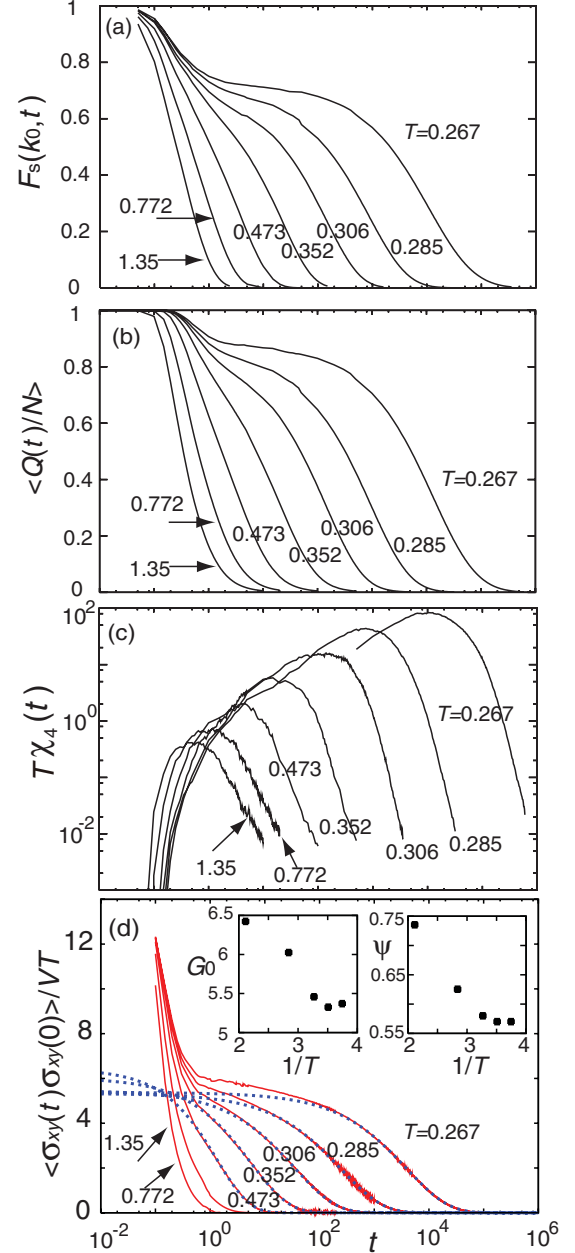

FIG. 1. (Color online) (a) $F_s^{(1)}(\boldsymbol{k}_0,t)$ at $|\boldsymbol{k}_0| = 2\pi$, (b) $\langle Q/N \rangle(t)$, (c) $\chi_4(t)$, and (d) $\langle \hat{\sigma}_{xy}(t)\hat{\sigma}_{xy}(0) \rangle/VT$ (red curves) for several temperatures. In (d), the long-time behavior of the stress autocorrelation can be well fitted by the KWW form, $G_0 \exp[-(t/\tau_\alpha^\sigma)^\psi]$ (blue dashed curves). The insets show the fitted parameters G_0 and ψ.

where $\boldsymbol{r}_{ij} = \boldsymbol{r}_i - \boldsymbol{r}_j$, $r_{ij} = |\boldsymbol{r}_{ij}|$, and m_i and $\boldsymbol{v}_i$ are the mass and velocity of the ith particle, respectively. Here, $\Phi(\boldsymbol{r}_{ij})$ is given by

$$\Phi(\boldsymbol{r}_{ij}) = \frac{r_{ij}}{2i\boldsymbol{k}\cdot\boldsymbol{r}_{ij}} \frac{\partial U_{ij}}{\partial r_{ij}}(e^{-i\boldsymbol{k}\cdot\boldsymbol{r}_i} - e^{-i\boldsymbol{k}\cdot\boldsymbol{r}_j}). \qquad (6)$$

The first term in Eq. (5) represents the momentum transfer contribution (ideal-gas term); it is negligibly small in comparison to the second term in the high-density liquid. Figure 1(d) shows the macroscopic shear stress autocorrelation function $\langle \hat{\sigma}_{xy}(t)\hat{\sigma}_{xy}(0) \rangle/VT$. In a supercooled state, the long-time behavior of $\langle \hat{\sigma}_{xy}(t)\hat{\sigma}_{xy}(0) \rangle/VT$ can be

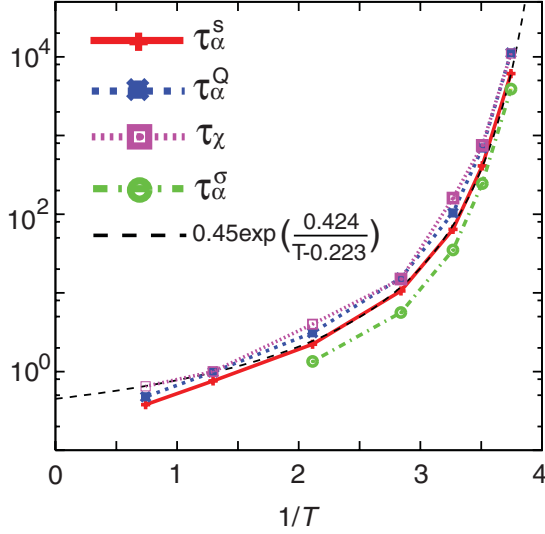FIG. 2. (Color online) τ_α^s, τ_α^Q, τ_χ, and τ_α^σ against $1/T$ are plotted by the red solid, blue dashed, purple dotted, and green dot-dashed curves, respectively. The thin black dashed curve is the fit of τ_α^s to the VFT law for $T \gtrsim 0.473$.

well fitted by the Kohlrausch-Williams-Watts (KWW) form, $G_0 \exp[-(t/\tau_\alpha^\sigma)^\psi]$, where G_0 is the plateau modulus and τ_α^σ is the structural relaxation time [25]. Nonexponential decay with the stretching exponent ψ has been considered to be a consequence of DH. Despite this nonexponential decay, the Maxwell relation, $\eta(k=0) \cong G_0 \tau_\alpha^\sigma$, holds well, even in a supercooled state [28]. In Fig. 2, we show four time scales, τ_α^s, τ_α^Q, τ_χ, and τ_α^σ. They behave similarly over the entire temperature range and follow the Vogel-Fulcher-Tammann (VFT) law. This amazing coincidence of the macroscopic structural relaxation time (τ_α^σ) with the microscopic relaxation time (τ_α^s and τ_α^Q), and also with the characteristic time of DH (τ_χ), apparently supports the MCT scenario, in which the slowing down of the particle dynamics as a result of the caging dominates the macroscopic transport anomalies and DH. Contrary to this coincidence, however, we will demonstrate below that the viscoelastic response of a supercooled liquid cannot be described by microscopic caging dynamics; rather, it involves the far more complicated heterogeneous dynamics of a mesoscopic length scale ξ.

IV. NONLOCAL VISCOELASTICITY

A. General formulation

To access the k dependence of the viscoelastic (structural) relaxation, we analyze the k-dependent complex modulus. We start from the following generalized hydrodynamic equation [23,24,29,30]:

$$\frac{\partial}{\partial t} \boldsymbol{j}^\perp = (\boldsymbol{\nabla} \cdot \overset{\leftrightarrow}{\boldsymbol{\sigma}}_{\text{vis}})^\perp + \boldsymbol{\theta}^\perp, \qquad (7)$$

where $\boldsymbol{j}^\perp(\boldsymbol{r},t)$ is the transverse momentum current, $\boldsymbol{\theta}^\perp(\boldsymbol{r},t)$ is the transverse random force, and $\overset{\leftrightarrow}{\boldsymbol{\sigma}}_{\text{vis}}(\boldsymbol{r},t)$ is the (transverse) viscous shear stress tensor given by $\overset{\leftrightarrow}{\boldsymbol{\sigma}}_{\text{vis}}(\boldsymbol{r},t) = \int dt' \int d\boldsymbol{r}' \eta(|\boldsymbol{r}-\boldsymbol{r}'|, t-t') \overset{\leftrightarrow}{\boldsymbol{\kappa}}{}^\perp(\boldsymbol{r}',t')$ with the strain rate

tensor $\overset{\leftrightarrow}{\boldsymbol{\kappa}}{}^\perp(\boldsymbol{r},t) = \boldsymbol{\nabla} \boldsymbol{v}^\perp + (\boldsymbol{\nabla} \boldsymbol{v}^\perp)^\dagger$. Here, $\boldsymbol{v}^\perp(\boldsymbol{r},t)$ is the transverse velocity, and $\eta(|\boldsymbol{r}-\boldsymbol{r}'|, t-t')$ is a response function representing the spatiotemporally nonlocal viscoelastic response. In the k space, the above equation is expressed as follows:

$$\frac{\partial}{\partial t} \boldsymbol{j}_{\boldsymbol{k}}^\perp(t) = -\frac{k^2}{\rho_m} \int dt' \eta(k, t-t') \boldsymbol{j}_{\boldsymbol{k}}^\perp(t') + \boldsymbol{\theta}_{\boldsymbol{k}}^\perp(t), \quad (8)$$

where ρ_m is the average mass density. Here, the Fourier transform of an arbitrary function $A(\boldsymbol{r})$ is defined by $A_{\boldsymbol{k}} = \int d\boldsymbol{r} e^{-i\boldsymbol{k}\cdot\boldsymbol{r}} A(\boldsymbol{r})$. The microscopic expression of $\boldsymbol{j}_{\boldsymbol{k}}^\perp(t)$ is given by $\boldsymbol{j}_{\boldsymbol{k}}^\perp(t) = 1/\sqrt{N} \sum_i^N m_i \boldsymbol{v}_i^\perp(t) e^{i\boldsymbol{k}\cdot\boldsymbol{r}_i(t)}$, where $\boldsymbol{v}_i^\perp(t)$ is the transverse velocity of particle i, which satisfies $\boldsymbol{v}_i^\perp(t) \cdot \boldsymbol{k} = 0$. The autocorrelation function is then defined as follows: $C(k,t) = \langle \boldsymbol{j}_{\boldsymbol{k}}^\perp(t) \cdot \boldsymbol{j}_{-\boldsymbol{k}}^\perp(0) \rangle$, whose time evolution is described by $(\partial/\partial t)C(k,t) = -(k^2/\rho_m) \int dt' \eta(k, t-t') C(k,t')$. Here, we make use of the relation $\langle \boldsymbol{\theta}_{\boldsymbol{k}}^\perp(t) \cdot \boldsymbol{j}_{-\boldsymbol{k}}^\perp(t') \rangle = 0$. In the frequency ($\omega$) domain, the resulting k- and ω- dependent shear viscosity can be expressed as follows:

$$\eta(k,\omega) = \frac{\rho_m}{k^2 \tilde{C}(k,\omega)} [-i\omega \tilde{C}(k,\omega) + C(k,0)], \qquad (9)$$

where $\tilde{C}(k,\omega) = \int_0^\infty dt e^{-i\omega t} C(k,t)$. The nonlocal viscoelasticity is characterized by the complex shear modulus $G^*(k,\omega) = G'(k,\omega) + iG''(k,\omega) = i\omega \eta^*(k,\omega)$, where $G'(k,\omega)$ and $G''(k,\omega)$ are the so-called storage and loss moduli, respectively [31,32]: The storage modulus represents the elastic response, and the loss modulus represents the dissipative viscous response. In the low-frequency limit ($\omega \to 0$), we can obtain the following expression for the k-dependent shear viscosity:

$$\eta(k) = \lim_{\omega \to 0} \frac{G''(k,\omega)}{\omega} = \frac{\rho_m}{k^2} \left[\int_0^\infty dt \frac{C(\boldsymbol{k},t)}{C(\boldsymbol{k},0)} \right]^{-1}. \qquad (10)$$

B. Mesoscopic nature of the viscoelastic response

The behavior of the complex modulus $G^*(k,\omega)$ describes the transmission and propagation of force and velocity fluctuations. Figure 3 shows the complex shear modulus $G^*(k,\omega) = G'(k,\omega) + iG''(k,\omega)$ for different wave numbers at three temperatures. At a relatively high frequency ($\omega \gtrsim 1$), $G^*(k,\omega)$ exhibits only a weak k dependence for all T's; $G'(k,\omega)$ and $G''(k,\omega)$ increase by less than one order of magnitude with decreasing k. This dependence implies that the short time scale ($t \lesssim 1$) relaxation dynamics are dominated by random particle motions with little spatial correlation, which are thermally activated rather independently, for both normal and supercooled states. Thus, the high-frequency viscoelastic response is microscopic, and it only weakly depends on T. In contrast, at a relatively low frequency ($\omega \lesssim 1$), the viscoelastic response shows a strong k dependence in a supercooled state. As we can see in the right column of Figs. 3(b) and 3(c), the shoulder in the loss modulus becomes more evident and shifts to lower frequencies with decreasing k, eventually developing into a distinct peak that cannot be seen in the normal state ($T = 1.35$). This behavior suggests the growth of dynamical correlation and the resulting heterogeneous nature of the slow structural relaxation as the system approaches T_g. For $k\xi \gtrsim 1$, the viscoelastic relaxation (or response) time increases for
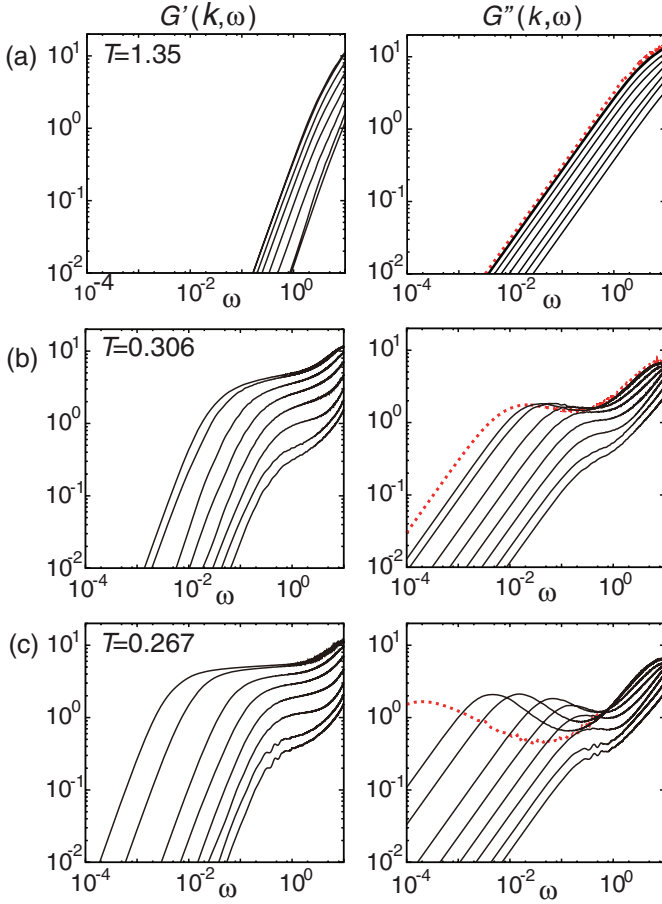
FIG. 3. (Color online) $G^*(k,\omega)$ at $k = 1.11$, 1.62, 2.64, 3.50, 4.35, 5.20, 6.05, and 6.91 (solid curves from left to right in each figure) in both the normal [(a) $T = 1.35$] and supercooled [(b) $T = 0.306$ and (c) 0.267] states. The storage and loss moduli are shown in the left and right columns, respectively. In the right column, the red dotted curves represent the loss modulus at $k = 0$.
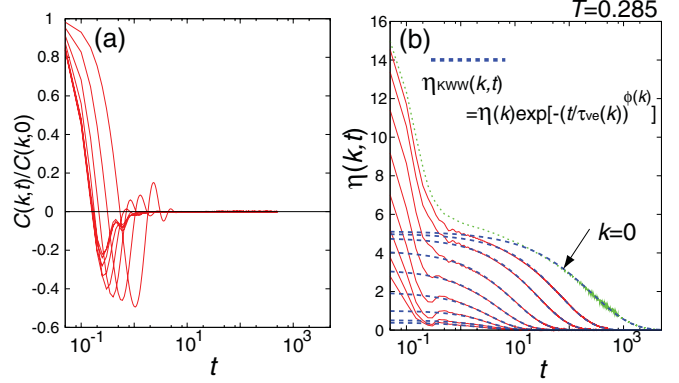

FIG. 4. (Color online) (a) The transverse momentum autocorrelation $C(k,t)$ and (b) the response function $\eta(k,t)$ at $T = 0.285$. In each figure, the red curves represent the data at $k = 1.11$, 1.62, 2.64, 3.50, 4.35, 5.20, 6.05, and 6.91 (from left to right). In (b), the blue dashed curves are the fits of the long-time behavior of $\eta(k,t)$ to the KWW function. The green dotted curve represents the macroscopic shear stress autocorrelation function.

longer length scales. For $k\xi \lesssim 1$, on the other hand, the viscoelastic response time coincides with the macroscopic relaxation time τ_α^σ [see also Fig. 5(b)].

To make a quantitative analysis in the time domain, we calculate the response function, $\eta(k,t)$, from $G^*(k,\omega)$ using the following relations: $G'(k,\omega) = \omega \int_0^\infty dt\,\eta(k,t)\sin(\omega t)$ and $G''(k,\omega) = \omega \int_0^\infty dt\,\eta(k,t)\cos(\omega t)$. Then, we fit $\eta(k,t)$ to the k-dependent KWW model, $\eta_{KWW}(k,t) = G_{ve}(k)\exp\{-[t/\tau_{ve}(k)]^\psi\}$, where $G_{ve}(k)$ and $\tau_{ve}(k)$ are the k-dependent plateau shear modulus and structural relaxation time, respectively [33]. This $\eta_{KWW}(k,t)$ reduces to the standard Maxwell model for $\psi = 1$. Figures 4(a) and 4(b) show the transverse momentum autocorrelation $C(k,t)$ and the response function $\eta(k,t)$ in a supercooled state ($T = 0.285$), respectively. Interestingly, $C(k,t)$ decays much faster than $\eta(k,t)$ for all wave numbers, though $C(k,t)$ and $\eta(k,t)$ are related by Eq. (9).

As shown in Fig. 5(a), $G_{ve}(k)$ has already assumed its macroscopic value, G_0, at a wavelength comparable to the particle size. This phenomenon can also be confirmed by the fact that neither the plateau of $G'(k,\omega)$ nor the peak height of $G''(k,\omega)$ depends on k when $k \lesssim 4$ [see Figs. 3(b)

and 3(c)]. Unlike $G_{ve}(k)$, $\tau_{ve}(k)$ exhibits a marked k dependence, as shown in Fig. 5(b). Its k dependence is characterized by the length scale $\xi_\tau \cong \xi$, which implies that the shear stress is dominated by the velocity fluctuations over distances of $\sim\xi$ and times of $\sim\tau_\alpha^\sigma = \tau_{ve}(0)$. Furthermore, unlike the weak T dependence of $G_{ve}(k)$, $\tau_{ve}(k)$ shows a dramatic increase with decreasing T. Thus, the mesoscopic nature of the viscoelastic response stems from $\tau_{ve}(k)$, but not from $G_{ve}(k)$. In Fig. 5(c), we compare $\eta(k)$ with $G_{ve}(k)\tau_{ve}(k)$ at several temperatures. In high-temperature normal-liquid states ($T \gtrsim 0.772$), $\eta(k)$ approaches its macroscopic ($k = 0$) value with a decrease in k, already at a wavelength comparable to the particle size [30]. This result suggests that there is no important length scale beyond the cage size in a normal-liquid state. In contrast, the k dependence of $\eta(k)$ becomes more pronounced for lower T in supercooled states ($T \lesssim 0.352$) [21,34,35]. We have found that the k-dependent Maxwell relation, $\eta(k) = G_{ve}(k)\tau_{ve}(k)$, holds well from the macroscopic to the microscopic length scale, irrespective of the degree of supercooling. The Maxwell relation does not hold if we employ the relaxation time of a variable linked to a longitudinal mode, such as the density ρ, as the structural relaxation time. For $\tau_\rho(k)$, which is the decay time of the two-body density correlation $\langle\rho(\boldsymbol{k},t)\rho(-\boldsymbol{k},0)\rangle$, we confirm that $\eta(k) \ll G_{ve}(k)\tau_\rho(k) \sim \eta(k = 0)$ for $k\xi \gtrsim 1$ [38]. This confirmation tells us that shear viscosity, which is the transport coefficient of a transverse velocity field, is proportional to the structural relaxation time for a purely transverse deformation at any k, but not one that involves longitudinal modes.

C. Comparison with the standard MCT

In this subsection, we consider whether our findings can be explained in the framework of the standard MCT [4,36,37]. MCT assumes that the dominant stress (or force density) is produced by density fluctuations. In a supercooled state, density fluctuations with wavelengths near the first peak of the structure factor ($\sim$cage size) become the longest-lived modes. Thus, their nonlinear (jamming)
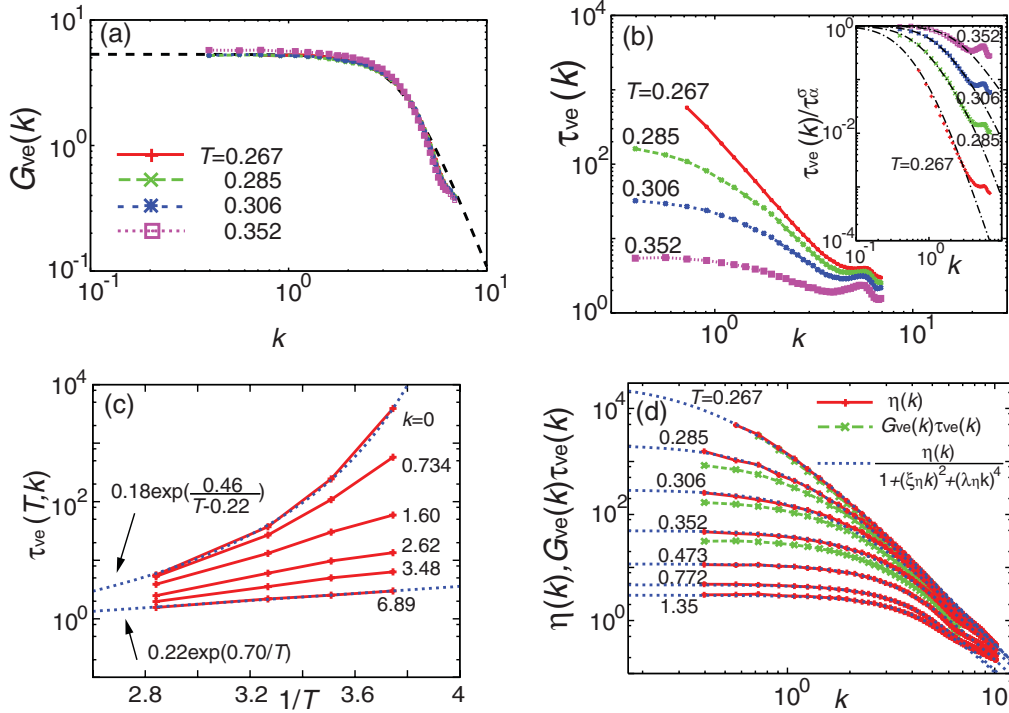
FIG. 5. (Color online) (a) The k-dependent plateau modulus $G_{ve}(k)$ in supercooled states. (b) The k-dependent relaxation time $\tau_{ve}(k)$ in supercooled states. The inset shows $\tau_{ve}(k)/\tau_{\alpha}^{\sigma}$. Here, the dot-dashed curve is the empirical function, $1/[1 + (\xi_{\tau}k)^2 + (\lambda_{\tau}k)^4]$, fitted to the data. (c) T dependence of $\tau_{ve}(k,T)$ for different values of k. The upper and lower blue dashed curves represent Vogel-Fulcher and Arrhenius fitting, respectively. (d) The k-dependent shear viscosity $\eta(k)$ (red curves). $\eta(k)$ can be well fitted by the empirical function, $\eta(k = 0,T)/\{1 + [\xi_{\eta}(T)k]^2 + [\lambda_{\eta}(T)k]^4\}$ (blue dashed curves), where $\eta(k = 0,T)$ is the macroscopic shear viscosity independently obtained by the Green-Kubo formula, and $\xi_{\eta} \cong \xi_{\tau}$. The green dashed curves represent $G_{ve}(k)\tau_{ve}(k)$ in supercooled states.

interactions are considered to play a crucial role in the slowing down of dynamics and the resulting transport anomalies. In our previous paper [21], our simple MCT analysis predicted that a viscosity anomaly occurs at a particle scale ($\sim$cage size) and that the crossover length remains nearly constant, regardless of the degree of supercooling. This prediction is, however, in strong contrast with our MD simulation results. As shown in Fig. 5(c), the viscosity anomaly in a supercooled state exhibits a marked k dependence for $k\xi \gtrsim 1$, where ξ increases as the degree of supercooling increases. Here, we further investigate the length-scale-dependent viscoelasticity within the framework of the standard MCT and compare it with the MD simulation results of $\eta(k,\omega)$. To capture the basic feature of the viscoelasticity in the MCT picture, we compute $\eta(k,\omega)$ of a one-component hard-sphere system, rather than a binary soft-sphere system.

The following fluctuating hydrodynamic equations provide a starting point:

$$m\frac{\partial}{\partial t}\hat{\rho} = -\nabla \cdot \hat{\boldsymbol{j}}, \tag{11}$$

where m is the particle mass, $\hat{\rho}(\boldsymbol{r},t)$ is the number density, and $\hat{\boldsymbol{j}}(\boldsymbol{r},t)$ is the momentum density, which obeys the following nonlinear Langevin equation:

$$\frac{\partial}{\partial t}\hat{\boldsymbol{j}} = -\hat{\rho}\nabla\frac{\delta F}{\delta\hat{\rho}} - \frac{\zeta_0}{m\rho_0}\hat{\boldsymbol{j}} + \hat{\boldsymbol{\theta}}, \tag{12}$$

where ζ_0 is the friction constant, ρ_0 is the average density, m is the particle mass, and $\hat{\boldsymbol{\theta}}$ is the thermal fluctuating force that satisfies the fluctuation-dissipation relation. The free energy functional $F\{\hat{\rho}\}$ is assumed to have the following expression:

$$F\{\hat{\rho}\} = k_B T \int d\boldsymbol{r}\,\hat{\rho}\left[\ln\left(\frac{\hat{\rho}}{\rho_0}\right) - 1\right]$$
$$- \frac{k_B T}{2} \int\int d\boldsymbol{r}d\boldsymbol{r}'\hat{c}(\boldsymbol{r}-\boldsymbol{r}')\delta\hat{\rho}(\boldsymbol{r})\delta\hat{\rho}(\boldsymbol{r}'), \tag{13}$$

where $\delta\hat{\rho} = \hat{\rho} - \rho_0$, and the direct correlation function and the structure factor are connected with the Ornstein-Zernike relation as $\rho_0\hat{c}_{\boldsymbol{k}} = 1 - 1/\hat{S}_{\boldsymbol{k}}$. In a hard sphere system, the structure factor is evaluated by the Percus-Yevick theory [23]. The wavelength corresponding to the first peak of the structure factor provides the characteristic size of the system ($\sim$cage size) [see Fig. 6(a)]. In this subsection, we measure space and time in units of d and $\zeta_0 d^2/\rho_0 k_B T$, respectively, where d is the particle diameter. Then, the viscosity is measured in units of $\zeta_0/\rho_0 d$. The k- and ω-dependent shear viscosity $\hat{\eta}(k,\omega)$ can be calculated by the Green-Kubo formula with the usual mode coupling approximation [4] as

$$\hat{\eta}(k,\omega) = \frac{1}{4k^2}\int_0^{\infty} dt e^{-i\omega t}\int_{\boldsymbol{p}}\left[p^2 - \left(\frac{\boldsymbol{k}\cdot\boldsymbol{p}}{k}\right)^2\right]$$
$$\times\left(\frac{1}{\hat{S}_p} - \frac{1}{\hat{S}_{|\boldsymbol{k}-\boldsymbol{p}|}}\right)^2\hat{S}_p\hat{S}_{|\boldsymbol{k}-\boldsymbol{p}|}\hat{\Psi}_p(t)\hat{\Psi}_{|\boldsymbol{k}-\boldsymbol{p}|}(t), \tag{14}$$
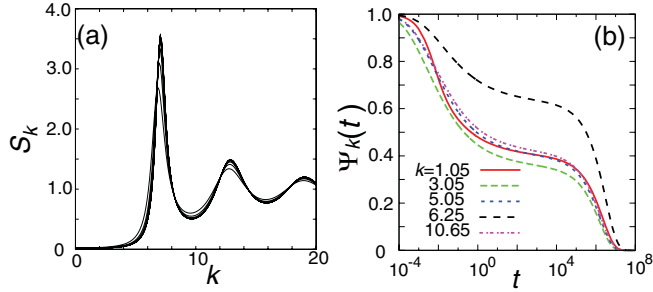
FIG. 6. (Color online) MCT results. (a) The structure factor $S_k = \langle|\hat{\rho}_k|^2\rangle/N$ for several volume fractions $\varphi = \pi d^3 \hat{\rho}_0/6 = \varphi_c(1 - 10^{-n/3})$, where $\varphi_c \cong 0.516$ and $n = 3, 4, \ldots, 12$. Notice that S_k collapses onto a single curve for $n \geqslant 7$. (b) The density autocorrelation function $\Psi_k(t)$ at $n = 11$ for several wave numbers.

where $\hat{\Psi}_k(t) = \langle\hat{\rho}_k(t)\hat{\rho}_{-k}(0)\rangle/\langle|\hat{\rho}_k|^2\rangle$. Figure 6(b) shows $\hat{\Psi}_k(t)$ at different wave numbers in a supercooled state. In the long-wavelength, low-frequency limit, Eq. (14) reduces to

$$\hat{\eta}_{\text{macro}} = \frac{1}{60\pi^2} \int_0^\infty dp\, p^4 \left(\frac{\partial}{\partial p} \ln \hat{S}_p\right)^2 \int_0^\infty dt\, \hat{\Psi}_p^2(t). \quad (15)$$

From the mathematical structure of the above integrals, the divergence of the viscosity is dominated by the density fluctuations with the wavelength around the first peak of the structure factor.

Figures 7(a) and 7(b) show the MCT results of the storage and loss moduli in supercooled states, respectively. No strong wave number dependence is apparent over the entire frequency range. As k decreases from 4.55 to 0.55, both $\hat{G}'(k,\omega)$ and $\hat{G}''(k,\omega)$ change by less than a factor of two; moreover, the position and height of the α peak in $\hat{G}''(k,\omega)$ remain nearly unchanged. In the standard MCT employed here, the viscoelastic response is dominated by the local cage-scale dynamics with little spatial correlation even for $\omega\tau_\alpha \lesssim 1$. Both the fast relaxation process and the slow structural relaxation have a microscopic origin. The results in Fig. 7 are indeed consistent with this MCT picture, but they are contradictory to the results of our MD simulation shown in Figs. 3–5. In MCT, the relation $\hat{\eta}_{\text{macro}} \sim \hat{\eta}(k) \sim \hat{\tau}_\rho(k)$ is qualitatively valid, even up to the particle scale. Here $\hat{\tau}_\rho(k)$ is the k-dependent α-relaxation time determined by $\hat{\Psi}_k(t)$. This result means that the longitudinal relaxation entirely dominates the transverse relaxation. Our MD result gives the generalized Maxwell relation as follows: $\eta(k) \sim \tau_{\text{ve}}(k) \ll \eta(k = 0) \sim \tau_\rho(k)$ for $k\xi \gtrsim 1$. This result strongly suggests the existence of a relaxation mechanism much faster than the longitudinal structural relaxation, which becomes important in the shear-stress relaxation on smaller length scales ($k\xi \gtrsim 1$). This strong separation of time scales between the longitudinal and transverse structural relaxations may be essential to the understanding of some unresolved problems, such as the breakdown of the Stokes-Einstein relation and the decoupling between translational and rotational dynamics in a supercooled state, which the standard MCT fails to explain. Recently, there have been several efforts to extend MCT to explain the growing length scale associated with DH [19,20]. Such approaches may help to resolve the discrepancies between our MD and the
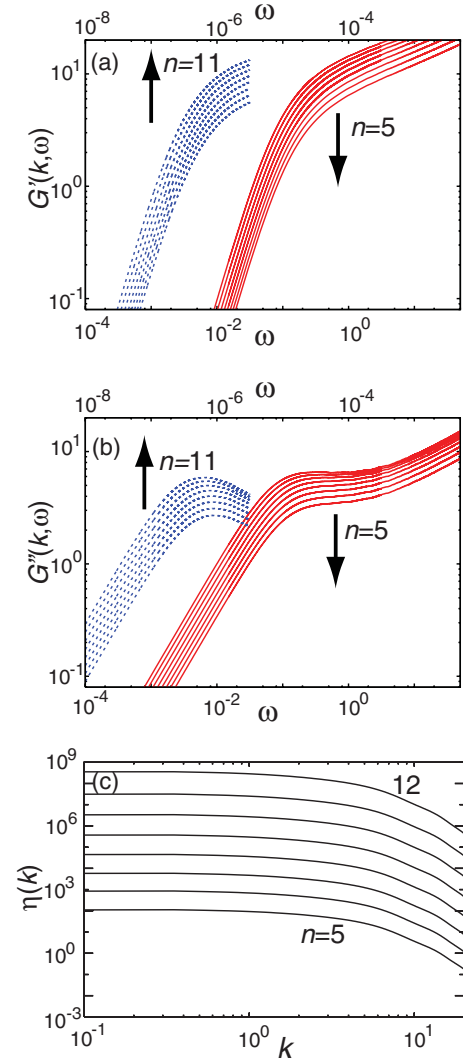

FIG. 7. (Color online) MCT results. The storage (a) and loss (b) moduli in supercooled states at $n = 5$ (red solid curves) and 11 (blue dashed curves) for different wave numbers ($k = 0.55, 1.05, 1.55, 2.05, 2.55, 3.05, 3.55$, and 4.05 from top to bottom). In (c), we show the k-dependent shear viscosity $\eta(k)$ at $n = 5, 6, \ldots, 12$ (from bottom to top).

(standard) MCT results. However, further investigation in this direction is beyond the scope of the present paper.

V. CONCLUDING REMARKS

In conclusion, we demonstrate that viscoelastic relaxation itself takes place heterogeneously in both space and time. The process involves particle rearrangements over the length scale ξ and takes τ_α^σ. The resulting relaxation time of a supercooled liquid τ_{ve} shows a marked k dependence. At a microscopic length scale, τ_{ve} always remains short and follows the Arrhenius law, whereas at a macroscopic length scale it slows down significantly with a decrease in T, following the VFT law. This behavior implies the intrinsically mesoscopic nature of the slow dynamics near the glass transition. The autocorrelation of the transverse variables at finite k itself decays much faster than τ_α^σ, which gives an impression that

the dynamics of the transverse modes at finite k are not linked to slow glassy dynamics. However, the analysis of $G^*(k,\omega)$ reveals the spatiotemporal hierarchical nature of the slow dynamics. This situation is similar to the case of entangled polymer solutions [41,42], which inspired this work. In that case, the marked k dependence of the relaxation time and the quick decay of transverse dynamics are direct consequences of dynamic coupling between the polymer and solvent dynamics. Our preliminary MCT calculation shows that the complex modulus takes the macroscopic value at a microscopic length scale over the whole frequency range, contrary to our findings. This discrepancy casts a doubt on the validity of the cage-based (particle-scale) scenario. The drastic slowing down of the microscopic relaxation time $\tau_\rho(k_p)$ could be a consequence of the subordination of the longitudinal modes to the mesoscopic slow structural relaxation with the timescale $\tau_{\rm ve}(k = 1/\xi) \sim \tau_\alpha^\sigma$. The most fundamental remaining question is that of the cause of slow structural relaxation of a mesoscopic nature.

[1] M. D. Ediger, C. A. Angell, and S. R. Nagel, J. Phys. Chem. **100**, 13200 (1996).

[2] P. G. Debenedetti and F. H. Stillinger, Nature (London) **410**, 259 (2001).

[3] K. Binder and W. Kob, *Glassy Materials and Disordered Solids* (World Scientific, Singapore, 2005).

[4] W. Götze, *Complex Dynamics of Glass-Forming Liquids: A Mode-Coupling Theory* (Oxford University Press, Oxford, 2009).

[5] H. Sillescu, J. Non-Cryst. Solids **243**, 81 (1999).

[6] M. D. Ediger, Annu. Rev. Phys. Chem. **51**, 99 (2000).

[7] E. R. Weeks, J. C. Crocker, A. C. Levitt, A. Schofield, and D. A. Weitz, Science **287**, 627 (2000).

[8] M. M. Hurley and P. Harrowell, Phys. Rev. E **52**, 1694 (1995).

[9] W. Kob, C. Donati, S. J. Plimpton, P. H. Poole, and S. C. Glotzer, Phys. Rev. Lett. **79**, 2827 (1997).

[10] R. Yamamoto and A. Onuki, Phys. Rev. E **58**, 3515 (1998).

[11] A. Onuki, *Phase Transition Dynamics* (Cambridge University Press, Cambridge, 2002).

[12] B. Doliwa and A. Heuer, Phys. Rev. Lett. **80**, 4915 (1998).

[13] N. Lačević, F. W. Starr, T. B. Schrøder, and S. C. Glotzer, J. Chem. Phys. **119**, 7372 (2003).

[14] H. Shintani and H. Tanaka, Nature Phys. **2**, 200 (2006).

[15] L. Berthier and G. Biroli, Rev. Mod. Phys. **83**, 587 (2011).

[16] F. Fujara, B. Geil, H. Sillescu, and G. Fleischer, Z. Phys. B **88**, 195 (1992).

[17] M. T. Cicerone and M. D. Ediger, J. Chem. Phys. **104**, 7210 (1996).

[18] L. Berthier, Phys. Rev. E **69**, 020201(R) (2004).

[19] G. Biroli, J.-P. Bouchaud, K. Miyazaki, and D. R. Reichman, Phys. Rev. Lett. **97**, 195701 (2006).

[20] K. S. Schweizer and E. J. Saltzman, J. Chem. Phys. **119**, 1181 (2003).

[21] A. Furukawa and H. Tanaka, Phys. Rev. Lett. **103**, 135703 (2009).

[22] D. C. Rapaport, *The Art of Molecular Dynamics Simulation* (Cambridge University Press, Cambridge, 2004).

[23] J. P. Hansen and I. R. McDonald, *Theory of Simple Liquids* (Academic Press, Oxford, 1986).

[24] J. P. Boon and S. Yip, *Molecular Hydrodynamics* (Dover, New York, 1991).

[25] A large part of the stress correlation decays very quickly, resulting in the plateau modulus $G_0(T)$ much smaller than $G_\infty(T)$. Here $G_\infty(T) = \langle \hat\sigma_{xy} \hat\sigma_{xy} \rangle / VT$ is a spontaneous elastic modulus [23,24]. On the contrary, $G_0(T)$ is related to the degrees of freedom which involve the long-term stored stress during structural relaxation. On a recent attempt to compute the plateau modulus of glasses from first principles, see Refs. [26,27].

[26] H. Yoshino and M. Mezard, Phys. Rev. Lett. **105**, 015504 (2010).

[27] G. Szamel and E. Flenner, Phys. Rev. Lett. **107**, 105505 (2011).

[28] $\int_0^\infty dt\, G_0 \exp[-(t/\tau_\alpha^\sigma)^\psi] = G_0 \tau_\alpha \Gamma(1/\psi)/\psi$, where Γ is the Gamma function. For example, at $T = 0.267\, \Gamma(1/\psi)/\psi \cong 1.61$, with $\psi = 0.57$.

[29] D. J. Evans, Phys. Rev. A **23**, 2622 (1981).

[30] W. E. Alley and B. J. Alder, Phys. Rev. A **27**, 3158 (1983).

[31] R. G. Larson, *The Structure and Rheology of Complex Fluids* (Oxford University Press, Oxford, 1999).

[32] M. Doi and S. F. Edwards, *Theory of Polymer Dynamics* (Oxford University Press, Oxford, 1986).

[33] Although the exponent ψ also depends on k, the present numerical data are not accurate enough to definitely determine its value (ψ strongly fluctuates). However, we found that ψ decreases and converges to the macroscopic ($k = 0$) value with decreasing k.

[34] J. Kim and T. Keyes, J. Phys. Chem. B **109**, 21445 (2005).

[35] R. M. Puscasu, B. D. Todd, P. J. Daivis, and J. S. Hansen, J. Chem. Phys. **133**, 144907 (2010).

[36] M. Fuchs, W. Götze, I. Hofacker, and A. Latz, J. Phys. Condens. Matter **3**, 5047 (1991).

[37] T. Franosch, M. Fuchs, W. Götze, M. R. Mayr, and A. P. Singh, Phys. Rev. E **55**, 7153 (1997).

[38] The k-dependent relaxation time of the incoherent intermediate scattering function behaves as $\sim 1/D_s k^2$ and $\sim \tau_\alpha$ for $k\ell^* \ll 1$ and $k\ell^* \gg 1$, respectively, where D_s is the self-diffusion coefficient and ℓ^* is the crossover length scale from Fickian to non-Fickian particle diffusion [18,39]. Also, ℓ^* is comparable to the characteristic size of DH. A similar crossover behavior can be observed in $\tau_\rho(k)$, which is the relaxation time of the coherent scattering function [40].

[39] L. Berthier, D. Chandler, and J. P. Garrahan, Europhys. Lett. **69**, 320 (2005).

[40] A. Furukawa (unpublished results).

[41] A. Furukawa, J. Phys. Soc. Jpn. **72**, 209 (2003); **72**, 1436 (2003).

[42] A. Furukawa, J. Chem. Phys. **121**, 9716 (2004).